J Nanostruct 16(2): 1576-1586, Spring 2026

RESEARCH PAPER

Design and Development of a Novel Plasma System for the Synthesis of Metal Nanoparticles from Chloride Solutions

Ibrahim Hammadi Frhan [1], Ahmed Mohammed Alrawi [2], Huthaifa. M. Yaseen [2], Marwan Abdulaziz Hassan [3], Baker Fawzi Abdallaha [4]*

[1] *Ministry of Education, Directorate of Anbar Education, Anbar, Iraq*

[2] *College of Education, University of Fallujah, Anbar, Iraq*

[3] *University of Anbar, Anbar, Iraq*

[4] *Department of Chemistry, College of Science, University of Anbar, Anbar, Iraq*

ARTICLE INFO

Article History:
Received 02 December 2025
Accepted 20 February 2026
Published 01 April 2026

Keywords:
Metal Chlorides
Nanometals
Nano
Nanoparticle
Plasma

ABSTRACT

A plasma-assisted system was developed based on US010213614B2 to synthesise metallic nanoparticles at high concentrations. Metal chloride solutions (1000–3000 ppm) are processed in batch mode, with electrodes and an argon gas jet generating plasma at the gas–liquid interface. This triggers reactions, visible by a colour change, that form stable nanoparticle suspensions, which are then isolated by centrifugation at 10,000 rpm. Using this system, a range of nanometals—including Ni, Cu, Mn, Co, Zn, Cr, Fe, and Cd—were successfully synthesised with medium to very small nanoscale dimensions. The produced nanometals were further incorporated into graphene oxide–based nanocomposites at a fixed graphene oxide–to–nanometal ratio of 10:1 and evaluated as gas-sensing materials for H_2S and NO_2 detection. The metal concentrations in the nanocomposites were quantified using flame atomic absorption spectroscopy (FAAS), yielding values between 441.2 and 1433 ppm. Structural, optical, and morphological characterisations were conducted using X-ray diffraction (XRD), UV–Vis spectroscopy, FAAS, and field-emission scanning electron microscopy (FESEM), confirming successful nanoparticle formation and crystallinity. The developed plasma system demonstrated high efficiency, reproducibility, and excellent control over nanoparticle size, offering a versatile platform for advanced nanomaterial synthesis and sensor applications.

How to cite this article
Frhan I., Alrawi A., Yaseen M, Hassan M, Abdallaha B. Design and Development of a Novel Plasma System for the Synthesis of Metal Nanoparticles from Chloride Solutions. J Nanostruct, 2026; 16(2):1576-1586. DOI: 10.22052/JNS.2026.02.009

INTRODUCTION

In recent decades, nanotechnology has attracted considerable interest from scientists across a wide range of disciplines due to the remarkable changes in material properties that occur when dimensions are reduced to the nanometer scale. As reported by Chattopadhyay and Patel, materials exhibit fundamentally different physical and chemical behaviours when at least one of their dimensions is confined to the nanoscale (1–100 nm) compared to their bulk counterparts [1]. When bulk materials are subdivided into nanoparticles, unexpected properties emerge as a result of quantum confinement effects and a significantly increased surface-to-volume ratio.Metal nanoparticles, in particular, have gained extensive attention

* *Corresponding Author Email: Ibrahim.hum69@gmail.com*

owing to their unique size-dependent properties and broad applicability in fields such as optics, magnetism, catalysis, sensing, and thermal and electronic devices [2]. The optical behavior of noble metal nanoparticles is primarily governed by the collective oscillation of conduction electrons induced by electromagnetic radiation, known as localized surface plasmon resonance (LSPR). This phenomenon is especially prominent in metals such as gold (Au), silver (Ag), and copper (Cu), which possess free conduction electrons [3]. According to Chattopadhyay and Patel (2009), the exceptional physicochemical characteristics of metal nanoparticles, distinct from their bulk phases, have driven intensive research in this area [4]. These properties arise mainly from their nanoscale dimensions and high surface energy. Among the various synthesis techniques, chemical reduction of metal ions in solution remains the most widely employed method for nanoparticle fabrication [5]. However, achieving precise control over particle size and morphology at the nanoscale remains a major challenge, as the underlying mechanisms governing size and shape evolution are not yet fully understood [6]. Nanotechnology, as a modern multidisciplinary field, enables the design and manipulation of materials with novel properties unattainable in their conventional forms, including enhanced surface area, electrical and thermal conductivity, mechanical strength, and improved transport behavior in biological systems [7]. Nanotechnology encompasses the integration of materials, tools, techniques, and human expertise aimed at producing and exploiting nanoscale structures for specific applications. Nanoparticles typically range from 1 to 100 nm in size, corresponding to dimensions on the order of 10^{-9} m [8,9]. Nanoscience has found extensive applications in medicine and pharmacies, industrial sectors such as nanosensors, energy storage devices, and solar cells, as well as agriculture through the development of nano-fertilizers and nano-pesticides. Additionally, nanocoatings are widely used to protect surfaces from corrosion and environmental degradation [10]. Metal nanoparticles, including platinum, gold, copper, cobalt, iron, and nickel, have demonstrated outstanding performance in catalysis, electronics, optics, antimicrobial applications, and biomaterials [11]. Their large specific surface area facilitates enhanced interaction with surrounding media, significantly improving catalytic efficiency and biological activity. Notably, nanoparticles synthesized via green routes using plant extracts are considered environmentally friendly and non-toxic, offering sustainable alternatives to conventional chemical methods [12]. Green synthesis approaches have gained prominence in recent years, particularly for biomedical applications such as biosensing and cancer therapy. Biogenic nanoparticles can interact effectively with proteins, antibodies, and intracellular components, enabling targeted therapeutic and diagnostic functions [13]. In addition to green methods, chemical techniques such as chemical vapor deposition (CVD) are widely used for producing thin films, especially in semiconductor industries [14]. Physical methods—including plasma synthesis, microwave irradiation, pulsed laser ablation, and gamma irradiation—are also employed for nanoparticle fabrication [15]. Nanotechnology has become an integral part of chemistry, physics, and engineering [16], as well as modern medicine, where it has contributed significantly to disease diagnosis, targeted therapy, and cost-effective healthcare solutions. Furthermore, nanomaterials are used in the development of nanodevices, biological nanostructures, nanorobots, and high-performance computing systems [17]. Nanoparticles can be synthesized using two fundamental approaches: top-down and bottom-up. The top-down approach involves breaking down bulk materials into nanoscale particles through mechanical or physical processes. In contrast, the bottom-up approach—often referred to as self-assembly—relies on the organization of atoms or molecules into well-defined nanostructures with superior physicochemical properties [18,19]. These advanced nanostructures offer enhanced performance and open new possibilities for future technological applications. In the biomedical field, nanotechnology has played a transformative role by enabling improved hemostatic materials for surgical applications, enhancing blood clotting processes, and facilitating the selective eradication of cancerous tumours while minimising damage to healthy cells [20].

MATERIALS AND METHODS

System parts

The system consists of an argon gas cylinder, which contains a regulator that controls the amount of gas output and its pressure, as well as a

flow meter, which controls the flow rate of the gas used and which passes through it to reach the gas jet needle, which is fixed on an iron stand.

A high voltage source of up to 5600 volts, which contains a voltage controller and a fan to cool the source coils. Two electrodes, one of which is connected to the gas jet needle (anode), while the other electrode (cathode) is in the form of a plate of metal that is a good electrical conductor. In a 50 ml beaker, the solution is placed in the middle, which contains the cathode electrode, and at a certain distance from the bottom of the beaker, so that the magnetic stone can be placed for the purpose of continuous stirring without it being attracted to the electrode. Electrical wires to connect the electrodes to the electrical circuit are coated with a thick insulating material. In addition, plastic tubes are used to deliver the gas from the source, through the flow meter, and then to the jet needle.

The hot plate, which is placed under the baker and at the bottom, and under the hot plate, is a mechanical controller to raise and lower the hot plate and the baker together to control the distance between the surface of the solution, and the gas jet needle with a distance not exceeding 2 cm. Through which plasma is effectively generated and when the gas is opened and the electrical circuit is closed, so that the flame is effective towards the solution (Fig. 1).

Plasma system design

The designed system is installed as shown

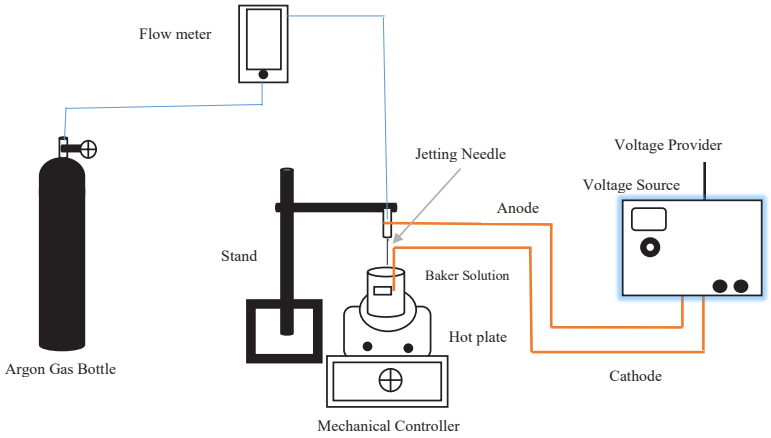

Fig. 1. A diagram showing the installation of the plasma system.

Fig. 2. Plasma system.

in Fig. 2. The gas is supplied from the Argon gas cylinder through plastic pipes at a pressure not exceeding 10 bar to the flow meter, which is fixed to the wall or to a well-fixed stand. The plastic tube is connected from the gas exit hole of the flow rate measuring device to the gas jet needle mounted on an iron stand, so that a good insulator is placed to prevent the needle from coming into contact with the iron stand. A conductive wire is connected to the jet needle to the voltage source as an anode.

The hot plate, which is fixed, is placed on a mechanical controller to raise or lower the hot plate. The hot plate is placed on the baker, which contains the solution, and the second electrode (cathode) is fixed in an appropriate manner. Fig. 3 shows the method of connecting the electrodes to the voltage source, which are placed inside the solution and connected with a metal wire to the source. Voltage and these wires are covered with thick insulation in order to avoid the danger of this voltage. In this way, the gas can be opened and the voltage source turned on, so that a plasma flame is formed on the surface of the solution.

Fig. 3. The process of installing the electrodes and the distance of the torch from the surface of the solution.

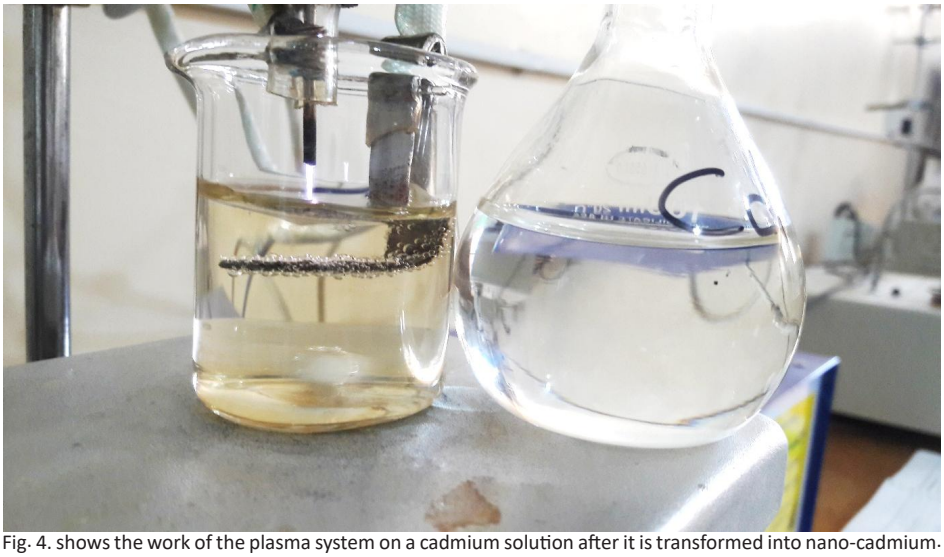

Fig. 4. shows the work of the plasma system on a cadmium solution after it is transformed into nano-cadmium.

Fig. 4 shows the operation of the plasma system on a white-colored cadmium chloride solution and its transformation after a short period into yellow-colored nano-cadmium. Likewise, Fis. 5 and 6 show the transformation of both copper and nickel into nano-copper and nano-nickel, respectively.

Practical part

The method of working on the system is carried out in the following steps:

1- Prepare solutions containing metals at a concentration of 1000 ppm to 3000 ppm, which are good concentrations to obtain appropriate quantities of nano-metals.

2- An appropriate amount of the prepared solution is placed in a 50 ml beaker, so that this quantity does not exceed 30 ml, and a magnetic stone is placed inside the solution for the purpose of continuous stirring while the torch is directed over the solution until the end of the process.

3- Opening the gas from its source so that the gas flow rate is 2 cm^3/s through a gas flow rate measuring device, and then opening the voltage source to its highest value, then the plasma flame

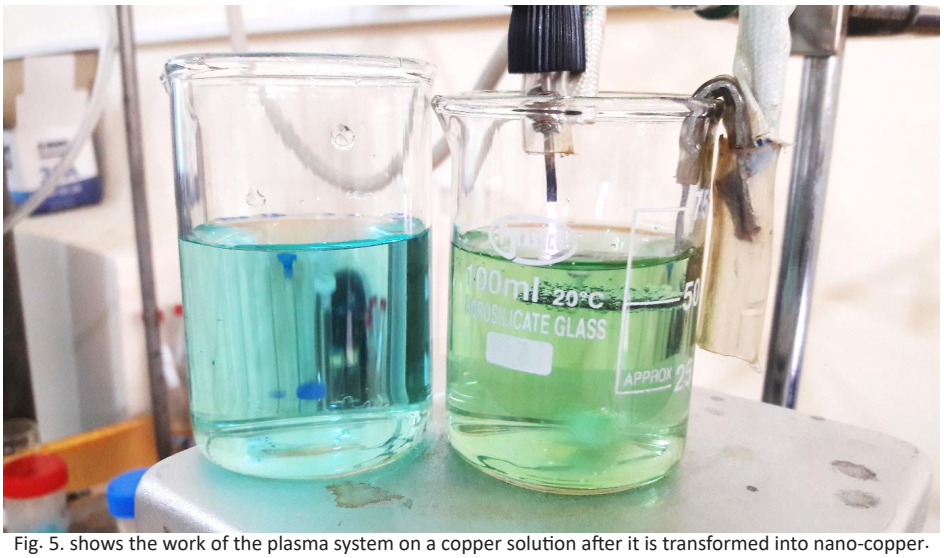

Fig. 5. shows the work of the plasma system on a copper solution after it is transformed into nano-copper.

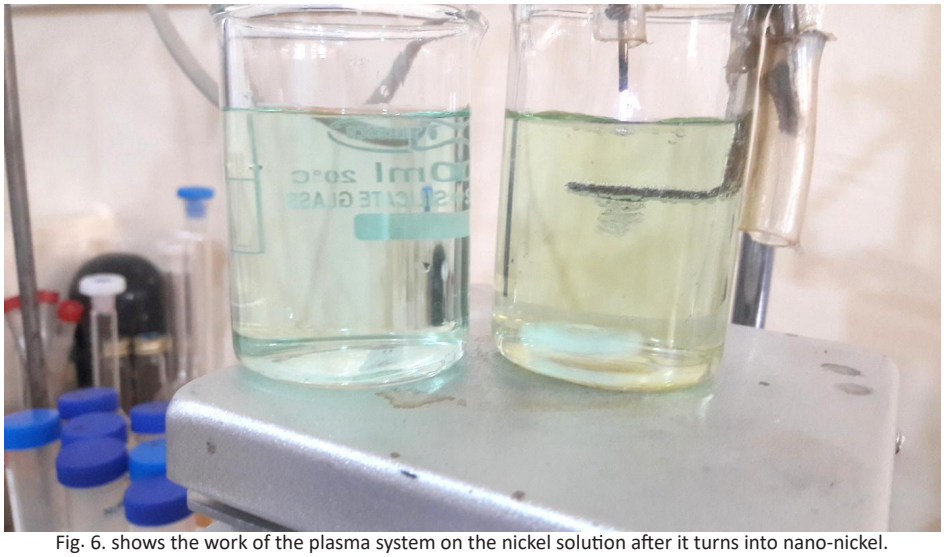

Fig. 6. shows the work of the plasma system on the nickel solution after it turns into nano-nickel.

will be generated.

4- Operating the motor through the hot plate for the purpose of continuous stirring, and through the manual controller, the baker placed on the hot plate .Can be raised to make the distance between the surface of the liquid in the baker, and the gas jet needle a distance of 2 cm, which is the distance at which the plasma is in its effective form.

5- With the passage of time, the color of the solution will gradually change until it reaches a different color. Then the voltage source can be turned off and the gas can be shut off at its source.

6- Repeat these steps until the prepared amount of solution runs out. The prepared quantities are collected in a large volumetric bottle for the purpose of separation.

7- These quantities are taken to separate the sediment from the filtrate by using a centrifuge (10,000 r/m). The sediment is collected after the filtrate is completely disposed of, and a small amount of distilled, deionized water is added to it.

8- These sediments, dissolved in distilled water, must be kept in a cool place away from light to protect them from oxidation processes.

9- These resulting deposits are nanoparticles of the metals that were prepared and can be confirmed by XRD examination as well as FESEM examination. These nanoparticles were later used to make nanocomposites with graphene oxide and use them as nanosensors for gases.

These processes were carried out at laboratory temperature and normal atmospheric pressure

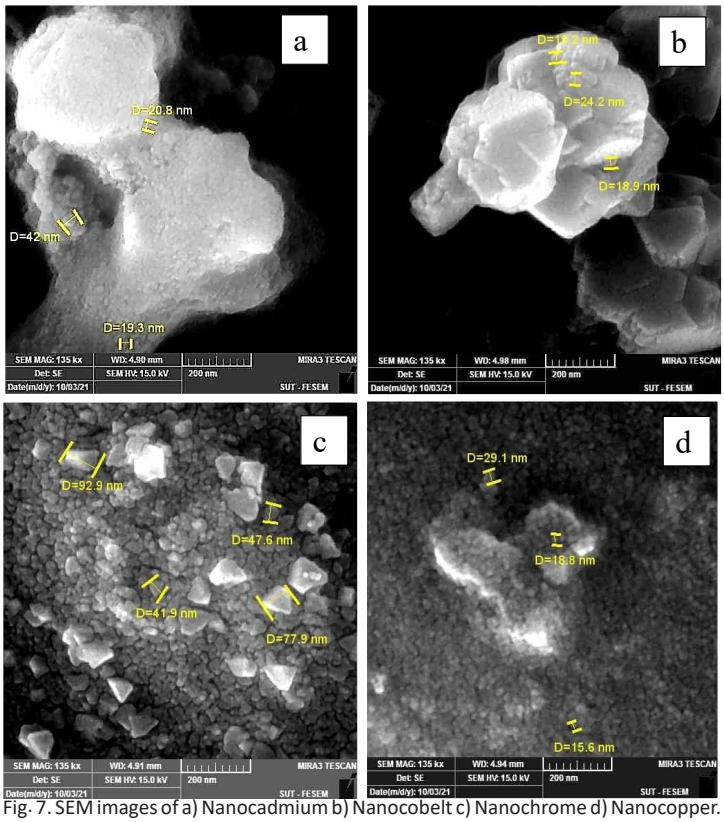

Fig. 7. SEM images of a) Nanocadmium b) Nanocobelt c) Nanochrome d) Nanocopper.

Table 1. Concentrations of nano-metals in ppm.

MNPs	Ni	Cu	Mn	Co	Zn	Cr	Fe	Cd
Con. ppm	500	688.9	369.2	441.2	533.7	554	1433	1022

without any hindrance, and high concentrations of the prepared metals were obtained, although there are differences in their deposition time and depending on the type of metal.

Materials used

Aqueous copper chloride ($CuCl_2.2H_2O$(, Nickel chloride ($NiCl_2$(, Zinc chloride ($ZnCl_2$), Aqueous chromium chloride ($CrCl_3.6H_2O$, Iron(III) chloride ($FeCl_3$), Aqueous manganese chloride ($MnCl_2.4H_2O$), Cadmium chloride ($CdCl_2$), Aqueous cobalt chloride ($CoCl_2.6H_2O$).

Diagnosis of the resulting nanometals

The resulting metal nanoparticles were characterized using a scanning electron microscope (FESEM). At Sharif University of Technology in Tehran, a Czech-made device was used to scan the surface of samples with a focused beam of electrons, which interfered with atoms in the sample to take the image. As well as the diagnosis of particles through XRD technology, these measurements were diagnosed in the Department of Science and Technology / Research Department in Baghdad, and the type of device was Japanese-made Shimadzu. It was done at ambient temperature to determine the crystalline size of the nanoparticles by using the Debye equation and knowing the identity of the elements. Using UV.vs technology with a wavelength of 200-800 nanometers and at ambient temperature, to determine the wavelengths of these particles. By using flame atomic absorption spectroscopy (FAAS) in the laboratories of the College of Science, Anbar University, and the resulting concentrations of these particles were determined and measured.

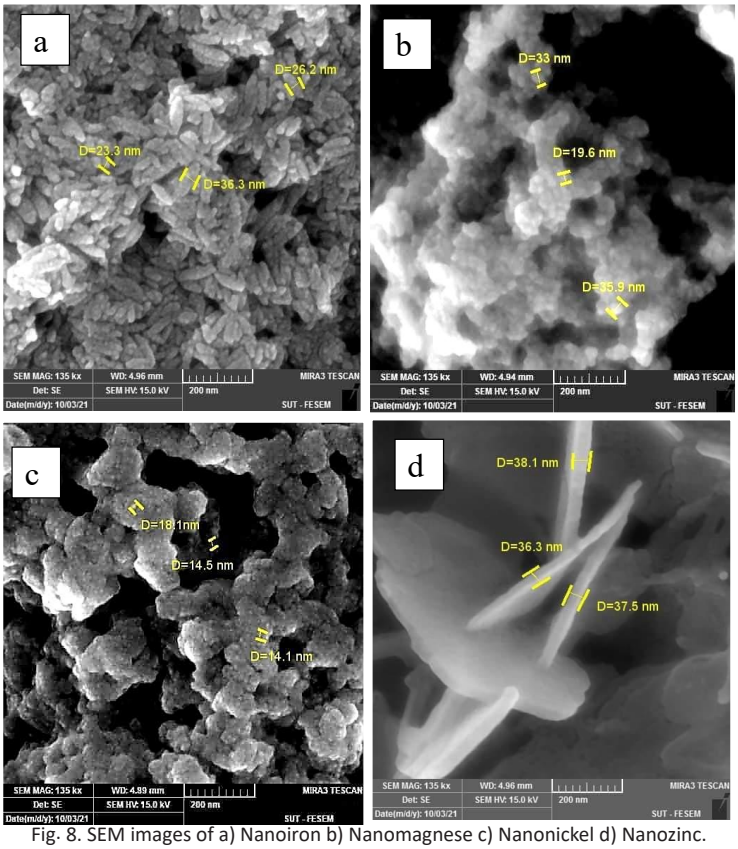

Fig. 8. SEM images of a) Nanoiron b) Nanomagnese c) Nanonickel d) Nanozinc.

Table 2. gives the wavelength values of nano-metals according to UV measurement.

MNPs	Ni	Cu	Mn	Co	Zn	Cr	Fe	Cd
W.L nm	275	310	520	450	285	375	341	190

RESULTS AND DISCUSSION

The system was used to prepare metal nanoparticles from their chloride salts under normal atmospheric pressure and laboratory temperature shown in Figs. S1-S8. Fig. S1 shows the transformation of cobalt chloride into nanocobalt and the color change from pink to brown [21]. As for Fig. S2 represents the transformation of chromium chloride into nanochromium and the color change from green to blackish green [22]. Fig. S3 shows the transformation of iron (III) chloride into nano-iron and the color changing from yellow to orange [23]. Fig. S4 shows the transformation of manganese chloride into nano-manganese and the color change from white to yellowish brown [24]. Fig. S5 shows the transformation of nickel chloride into nano-nickel and the color change from green to olive [25]. Fig. S6 represents the transformation

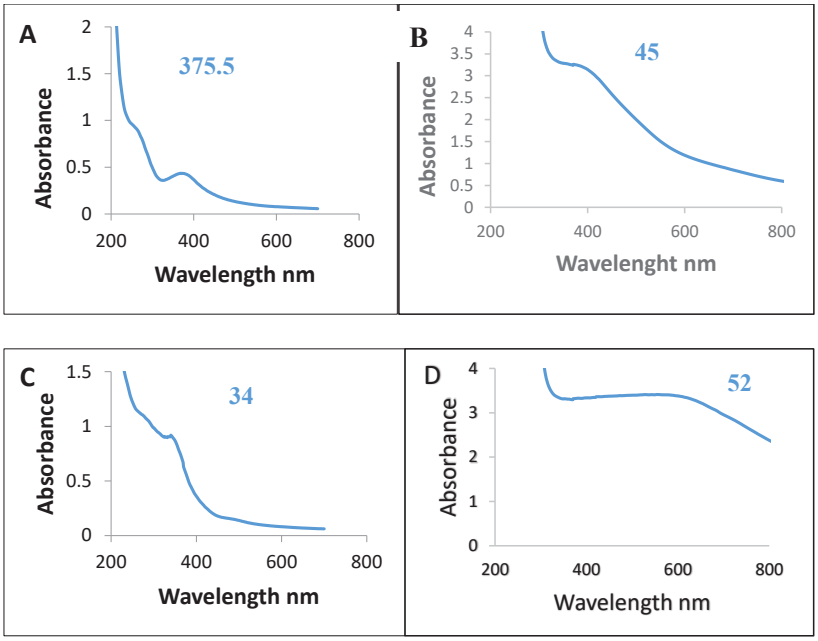

Fig. 9. UV-Vis spectrum of A) CrNPs B) CoNPs C) FeNPs D) MnNPs.

Table 3. Average crystallite size (D) of CrNPs and CoNPs.

Element	2 Theta (degree)	FWHM (degree)	Cos theta	FWHM (rad)	D (nm)	D Average
CrNPs	16.78	2.3616	0.98929	0.04121466	3.40587	13.875
	20.96	0.5904	0.98332	0.01030366	13.7063	
	22.92	1.1808	0.98006	0.02060733	6.87592	
	38.46	0.3936	0.94421	0.00686911	21.4110	
	65.06	0.3936	0.84313	0.00686911	23.9779	
CoNPs	16.89	0.5904	0.98915	0.01030366	13.6254	22.577
	20.87	0.3936	0.98346	0.00686911	20.5565	
	32.94	0.246	0.95897	0.00429319	33.7303	
	38.39	0.3936	0.94441	0.00686911	21.4065	
	61.85	0.3936	0.85786	0.00686911	23.5662	

of cadmium chloride into nano-cadmium and the color change from white to yellow [26]. Fig. S7 shows the transformation of zinc chloride into nano zinc and the color from white to brown. Fig. S8 represents the transformation of copper chloride into nano-copper and the color from blue to dark yellow [27]. The concentrations of metal nanoparticles were determined through FAAS technology, and Table 1 Shows the concentrations of these particles.

Nano-metals were identified using FESEM technology in the laboratories of Sharif University in Tehran using a Czech-made device at room temperature. The diameters of the cadmium (Cd) nanoparticles ranged between (19.3 nm - 42 nm) as in Fig. 7a. The diameters of cobalt (Co) particles range between 18.9 nm - 24.2 nm) as in Fig. 7b. Fig. 7c shows the diameters of chromium (Cr) metal particles, which are within the range (15.6 nm - 29.6 nm) and are the smallest diameters we obtained compared to particles of other metals. Fig. 7d represents the diameters of copper metal nanoparticles (Cu), which range from (41 nm - 77 nm) as an average of their nanoscopic diameters. The recorded diameters of iron (Fe) ranged between (32.3 nm -36.3 nm), as shown in Fig. 8a. The diameters of the manganese nanoparticles (Mn) ranged between (19.6 nm - 35.9 nm) as in Fig. 8b. In Fig. 8c, the diameters of nickel (Ni) nanoparticles appear and range between (14.1

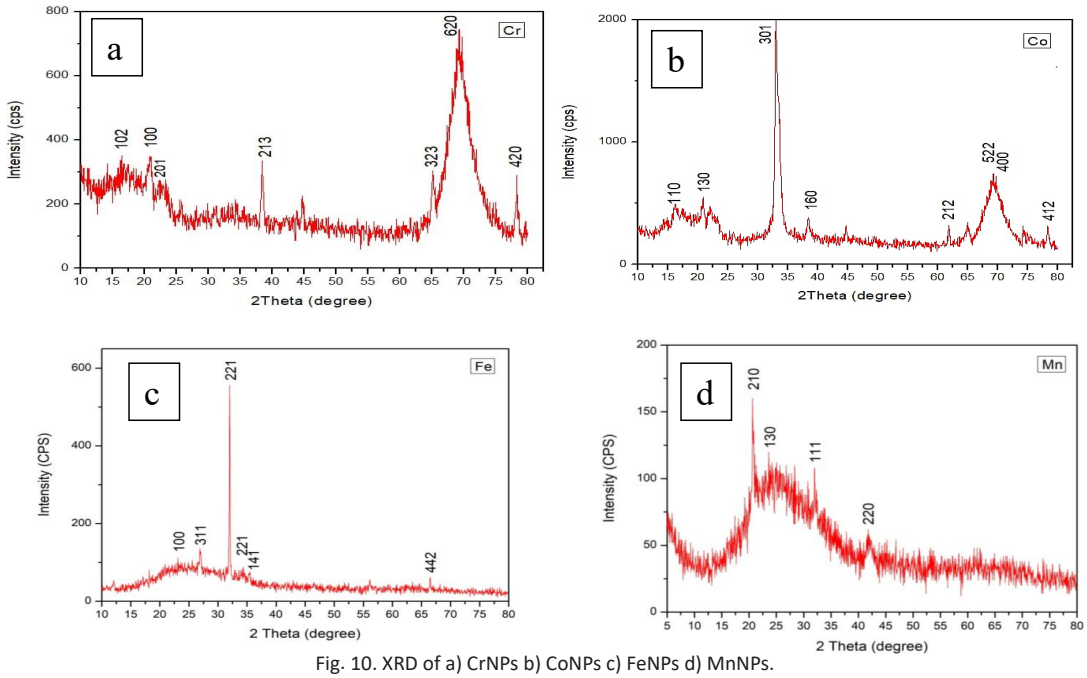

Fig. 10. XRD of a) CrNPs b) CoNPs c) FeNPs d) MnNPs.

Table 4. Average crystallite size (D) of FeNPs and MnNPs.

Element	2 Theta (degree)	FWHM (degree)	Cos theta	FWHM (rad)	D (nm)	D Average
FeNPs	22.62	0.17	0.980583	0.002967	47.734	56.483
	27.07	0.2886	0.972231	0.005036	28.359	
	32.15	0.1473	0.960905	0.002571	56.218	
	34.15	0.1487	0.955927	0.002595	55.979	
	66.53	0.1011	0.836166	0.001764	94.128	
MnNPs	20.81	0.61	0.983558	0.010646	13.262	12.253
	24.93	0.8	0.976431	0.013962	10.186	
	27.39	0.55	0.971573	0.009599	14.891	
	32.15	0.77	0.960905	0.013438	10.754	
	41.88	0.7	0.9339648	0.0122164	12.171	

nm - 18.1 nm). Fig. 8d represents the diameters of zinc (Zn) particles, which ranged between (36.3 nm - 38.1 nm). All of these particles were within the nanoscale range (1-100) nanometers.

Using UV.vs technology, a JASCO V 650 spectrophotometer was used to evaluate the absorption spectrum The results were obtained for the specific wavelengths of the peaks of the elements and were as follows: chromium (Cr=375.5nm), cobalt (Co=456nm), iron (Fe=341nm) and manganese (Mn=520nm). These wavelengths confirm the presence of nano-metals according to their density and size. Dependent on the beam area shown by the data (Fig. 9).

As for using XRD technology to determine the average crystal size of nanoparticles, the average crystal size ranged between (12.253 - 56.483) nanometers, as shown in Fig. 10, Tables 3 and Table 4, which are rates within the nanoscale. These particles were also identified through UV examination, and their wavelengths ranged between (190-520 nm), as shown in Table 2 of the nanoparticles formed in the wavelength range 200-800 nm with a resolution of 1 nm.

Through the tests conducted on metal nanoparticles and based on the above-mentioned values, sufficient evidence is given that these particles are in their nanoscopic form. This confirms that the system worked as required and well to obtain such nano-metals.

CONCLUSION

In conclusion, the described system effectively facilitates the generation of metal nanoparticles through a carefully designed setup involving an argon gas cylinder, high voltage source, and regulated flow mechanisms. By employing a sequential method that includes the use of metal chloride solutions at specified concentrations, the system successfully transforms these solutions into nanoparticles of various metals, exemplified by the distinct color changes observed. Characterization techniques such as FESEM, XRD, and UV-Vis spectrometry confirm the successful synthesis and properties of the nanoparticles, which fall within the nanoscale range and exhibit specific wavelengths corresponding to their respective metal compositions. The system operates efficiently under normal atmospheric conditions, yielding significant concentrations of metal nanoparticles that can subsequently be utilized in applications such as nanosensing. These findings illustrate the system's capability for producing high-quality nano-metals, supporting its potential for further research and industrial applications.

CONFLICT OF INTEREST

The authors declare that there is no conflict of interests regarding the publication of this manuscript.

REFERENCES

1. Kar S, Chaudhuri S. Cadmium Sulfide One-Dimensional Nanostructures: Synthesis, Characterization and Application. Synthesis and Reactivity in Inorganic, Metal-Organic, and Nano-Metal Chemistry. 2006;36(3):289-312.
2. Adul-Rasool AA, Athair DM, Zaidan HK, Rheima AM, Al-Sharify ZT, Mohammed SH, et al. 0,1,2,3D nanostructures, types of bulk nanostructured materials, and drug nanocrystals: An overview. Cancer Treatment and Research Communications. 2024;40:100834.
3. Gokulakrishnan J, Kamakshi K, Sekhar KC. Tuning the Morphological and Optical Properties of Pulsed Laser-Deposited Gold Nanoparticle Thin Films by Varying Number of Laser Pulses. Surface Engineering and Applied Electrochemistry. 2024;60(1):42-49.
4. Zhang X, Zhao N, He C. The superior mechanical and physical properties of nanocarbon reinforced bulk composites achieved by architecture design – A review. Prog Mater Sci. 2020;113:100672.
5. Marimuthu S, Kannan P, Maduraiveeran G. Transition metal sulfide nanostructures: synthesis and application in metal-air batteries. Nano Express. 2024;5(2):022005.
6. Harish V, Ansari MM, Tewari D, Yadav AB, Sharma N, Bawarig S, et al. Cutting-edge advances in tailoring size, shape, and functionality of nanoparticles and nanostructures: A review. Journal of the Taiwan Institute of Chemical Engineers. 2023;149:105010.
7. Malik S, Muhammad K, Waheed Y. Nanotechnology: A Revolution in Modern Industry. Molecules. 2023;28(2):661.
8. Suhag D, Thakur P, Thakur A. Introduction to Nanotechnology. Integrated Nanomaterials and their Applications: Springer Nature Singapore; 2023. p. 1-17.
9. Jana U, Mohanty AK, Pal SL, Manna PK, Mohanta GP. Felodipine loaded PLGA nanoparticles: preparation, physicochemical characterization and in vivo toxicity study. Nano Convergence. 2014;1(1).
10. Naskar S, Sharma S, Kuotsu K. Chitosan-based nanoparticles: An overview of biomedical applications and its preparation. J Drug Deliv Sci Technol. 2019;49:66-81.
11. Hanselman S, Koper MTM, Calle-Vallejo F. Using micro-solvation and generalized coordination numbers to estimate the solvation energies of adsorbed hydroxyl on metal nanoparticles. Physical Chemistry Chemical Physics. 2023;25(4):3211-3219.
12. Kharade S, Mane-Gavade S, Mali S, Shirote S, Malgave S, Nikam G. Biofabrication of Silver Nanoparticles Using Hibiscus cannabinus Leaf Extract and Their Antibacterial Activity. Macromolecular Symposia. 2020;393(1).
13. Choudhary S, Kumar R, Dalal U, Tomar S, Reddy SN. Green synthesis of nanometal impregnated biomass –

antiviral potential. Materials Science and Engineering: C. 2020;112:110934.
14. Raiford JA, Oyakhire ST, Bent SF. Applications of atomic layer deposition and chemical vapor deposition for perovskite solar cells. Energy and Environmental Science. 2020;13(7):1997-2023.
15. Khanna P, Kaur A, Goyal D. Algae-based metallic nanoparticles: Synthesis, characterization and applications. J Microbiol Methods. 2019;163:105656.
16. Muñoz-Écija T, Vargas-Quesada B, Chinchilla Rodríguez Z. Coping with methods for delineating emerging fields: Nanoscience and nanotechnology as a case study. Journal of Informetrics. 2019;13(4):100976.
17. Bale AS, Aditya Khatokar J, Singh S, Bharath G, Kiran Mohan MS, Reddy SV, et al. Nanosciences fostering cross domain engineering applications. Materials Today: Proceedings. 2021;43:3428-3431.
18. Chen H, Sun K, Tian Z, Shen C, Huang Y, Yan Y. BlendMask: Top-Down Meets Bottom-Up for Instance Segmentation. 2020 IEEE/CVF Conference on Computer Vision and Pattern Recognition (CVPR); 2020/06: IEEE; 2020. p. 8570-8578.
19. Tripathi RM, Chung SJ. Biogenic nanomaterials: Synthesis, characterization, growth mechanism, and biomedical applications. J Microbiol Methods. 2019;157:65-80.
20. Kuo SP, Tarasenko O, Chang J, Popovic S, Chen CY, Fan HW, et al. Contribution of a portable air plasma torch to rapid blood coagulation as a method of preventing bleeding. New Journal of Physics. 2009;11(11):115016.
21. Tarannum N, Kumar D, Kumar N. β-Cyclodextrin-Based Nanocomposite Derivatives: State of the Art in Synthesis, Characterization and Application in Molecular Recognition. ChemistrySelect. 2022;7(22).
22. Mahmoud W, Fayek A, taha a, El-Sherif A. Chromium complex nanoparticles sensor for arsenic detection using QCM technique. Egyptian Journal of Chemistry. 2023;0(0):0-0.
23. Lu Y, Dong W, Wang W, Wang Q, Hui A, Wang A. A comparative study of different natural palygorskite clays for fabricating cost-efficient and eco-friendly iron red composite pigments. Applied Clay Science. 2019;167:50-59.
24. Munir R, Ali K, Naqvi SAZ, Muneer A, Bashir MZ, Maqsood MA, et al. Green metal oxides coated biochar nanocomposites preparation and its utilization in vertical flow constructed wetlands for reactive dye removal: Performance and kinetics studies. J Contam Hydrol. 2023;256:104167.
25. Saravanakumar S, Saravanan R, Sasikumar S. Effect of sintering temperature on the magnetic properties and charge density distribution of nano-NiO. Chemical Papers. 2014;68(6).
26. El-Malawy D, Al-Abyad M, El Ghazaly M, Abdel Samad S, Hassan HE. γ-ray effects on PMMA polymeric sheets doped with CdO nano particles. Radiat Phys Chem. 2021;184:109463.
27. Abd E-Aty M, Ghazal H. Nanotechnology and Application of Nano Titanium Dioxide, Nano Zinc Oxide, and Nano Copper Oxide on Textile for High Performance. Egyptian Journal of Chemistry. 2022.